

## Stable isotope thermometry of the Nanga Parbat-Haramosh Massif and the Kohistan-Ladakh arc, northern Pakistan

MUHAMMAD U.K. KHATTAK<sup>1</sup>, DEBRA S. STAKES<sup>2</sup>, JOHN W. SHERVAIS<sup>3</sup>,  
MUHAMMAD ARIF<sup>4</sup> & M. TAHIR SHAH<sup>1</sup>

<sup>1</sup>National Center of Excellence in Geology, University of Peshawar, Pakistan

<sup>2</sup>Monterey Bay Aquarium Research Institute, 160 Central Ave., Pacific Grove, CA 93950, USA

<sup>3</sup>Department of Geological Sciences, University of South Carolina, Columbia, SC 29208, USA

<sup>4</sup>Department of Geology, University of Peshawar, Pakistan

**ABSTRACT:** *The Nanga Parbat-Haramosh Massif in northern Pakistan represents the northernmost exposure of the Indian plate that have been metamorphosed in the Late Tertiary subsequent to the Himalayan collision and overthrusting of the Asian plate onto the Indian plate. The massif a complex mixture of parag- and orthogneisses, of minor metabasics and calc-silicate rocks, and of post-metamorphic pegmatite dikes. The <sup>18</sup>O geothermometry results indicate that these gneisses are metamorphosed under peak temperatures of 700+°C.*

*The <sup>18</sup>O isotopic compositions of the rocks and their constituent minerals in the massif and adjacent areas of the Kohistan and Ladakh arc along the Indus and Astore Rivers vary as following: whole rock  $\delta^{18}\text{O}_{\text{SMOW}}=7\text{-}15.3\text{‰}$ ; quartz=7.4-16.4‰; feldspar=7-16.1‰; garnet=5.3-13.7‰; biotite=3.9-12.6‰; muscovite=6.7-12.7‰; and hornblending amphibole=4.4-7.2‰. The majority of the mineral  $\delta$ -values follow the "normal" sequence. <sup>18</sup>O thermometry results were calculated from <sup>18</sup>O fractionations among quartz, garnet, feldspar, biotite, muscovite and amphibole. Fifteen of the sixteen fractionations of Qtz-Gar-pairs ( $\alpha_{\text{QO}}$ ) vary from 2.8‰ to 3.8‰ giving a range of temperatures from 764°C to 599°C respectively. The 1.0‰ variation in fractionation is greater than the expected error and thus indicates a real variation in the maximum temperatures. Among the analyzed minerals, the feldspars, which are isotopically least stable, indicate isotopic resetting during a later event.*

### INTRODUCTION

The Himalayan mountain range, which extends from Afghanistan in the west to Burma in the east (Fig. 1), is the surface expression of collision between the Indian and Asian plates which closed the Neotethyan ocean at about 55 Ma (Powell, 1979). This collision caused the leading edge of the Indian plate to be intensely deformed

and greatly thickened, faulted, regionally metamorphosed, and intruded by post-collisional, anatectic granites. In northern Pakistan, an intra-oceanic island arc, the Kohistan-Ladakh Island Arc (KLIA), is sandwiched between the Asian and Indian plates. The Nanga Parbat-Haramosh Massif (NPHM), a NNE-trending unique geologic feature of the Himalayas of northern Pakistan, is thrust up from underneath

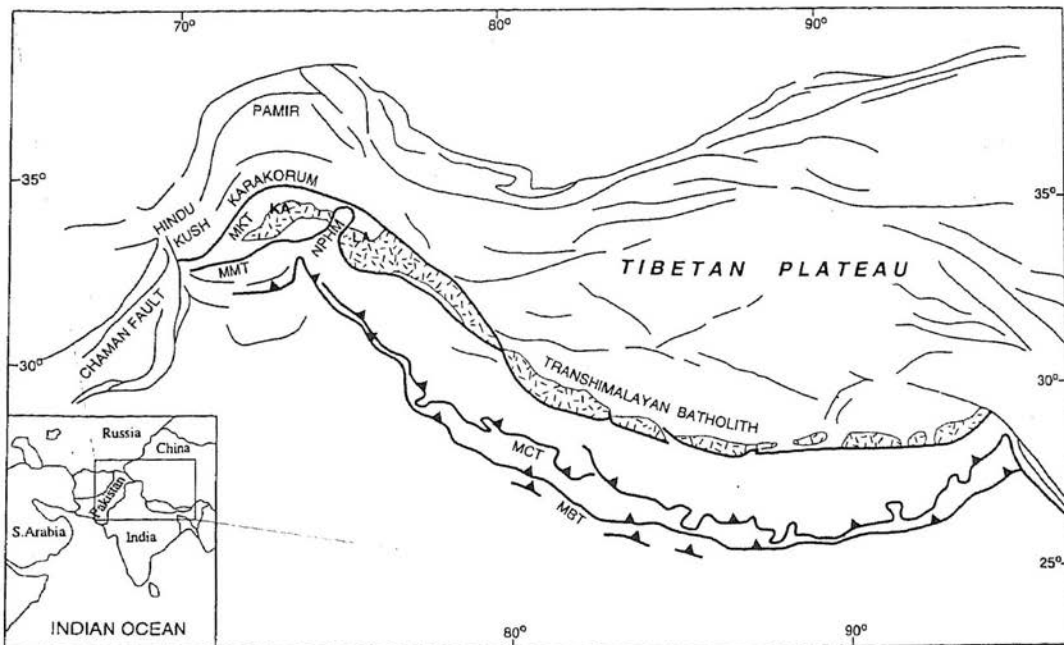


Fig. 1. Generalized tectonic map of the Himalayas. KA=Kohistan arc; LA=Ladakh arc; NPHM=Nanga Parbat-Haramosh Massif; MBT=Main Boundary Thrust; MCT=Main Central Thrust; MMT=Main Mantle Thrust; MKT=Main Karakoram Thrust (redrawn after Zeitler et al., 1991)

the KLIA rocks (Fig. 1). Recent geothermobarometric studies show that NPHM followed an increasing P-T and KLIA a decreasing P-T path (Khattak, 1990; Khattak & Stakes, 1993).

This study concerns the  $^{18}\text{O}$  isotope geothermometry of rocks from the massif and adjacent areas of the Kohistan and Ladakh arc. We have used  $^{18}\text{O}$  fractionations among contemporaneous mineral pairs to estimate the temperatures of formation of these assemblages during the last metamorphism in NPHM. The use of mineral pairs in thermometry is useful because it is independent of the isotopic composition of the metamorphic fluid and the absolute value of the minerals themselves. It is only dependent on the difference in isotopic value between the two contemporaneous minerals. Stable isotope geothermometry is a superior comparison to mineralogical geothermometers in that the fraction-

ation is independent of the pressures involved. This research is aimed at independently estimating the peak temperatures at the time of metamorphism and to make a petrogenetic interpretation of the *Ky/Sill* grade metamorphic rocks of the massif.

#### REGIONAL SETTING OF THE NPHM

In the northwestern Himalayas, a northern suture or Main Karakoram Thrust (MKT) and a southern suture or Main Mantle Thrust (MMT) enclose a deformed Cretaceous island arc, the KLIA, which is intruded by the calc-alkaline rocks, named as the Kohistan-Ladakh batholith. The Kohistan arc overrode the Indian plate during the Eocene, forming the MMT as well as other thrusts to the south (Fig. 1). South of the MMT are rocks of the Indian plate. The dominant rock-types are pelitic, calcareous and

psammitic metasediments of Precambrian to Early Eocene age that are extensively intruded by granites (Tahirikheli et al., 1979a). The metamorphic grade and the deformational intensity decreases from kyanite/sillimanite grade adjacent to the MMT to chlorite grade slates and weakly deformed mudstones in the south (Tahirikheli et al., 1979a).

The western boundary of the NPHM is the NNE-trending Raikot-Sassi "dextral reverse" fault zone (Fig. 2; Lawrence & Ghauri, 1983), which truncates the MMT south of Raikot. The trace of this steep thrust fault zone is characterized by a 2-2.5 km discontinuous band of mylonite (in some places hydrothermally metasomatized), hot springs, and numerous minor reverse faults, some of which are active (Lawrence & Ghauri, 1983; Madin, 1986; Butler & Prior, 1988; Butler et al., 1989). The southern extent of the fault zone is not known. This fault more or less follows the trace of MMT between Raikot and Sassi. To the west of the fault zone are exposed rocks of the Kohistan arc, with local lenses of the Kohistan arc material brought up along with MMT. The eastern boundary of the NPHM is the Astak Fault Zone (Fig. 2; Verplanck, 1986), which lies to the east of the suture between the Indian and Kohistan plates in western Ladakh. The sense of movement on this fault is sinistral-normal (i.e. west-side-up along KKH). To the east of the Astak Fault Zone lies the Ladakh terrane, which extends eastward through Ladakh into southern Tibet (Fig. 1). The eastern boundary of the massif is marked by significant changes in lithology, from interlayered dominantly metasedimentary lithologies on the west to strongly deformed complex zone of meta-igneous and metasedimentary rocks of the Ladakh arc on the east. This boundary is a zone about 5 km wide characterized by a complex of slices of rock-bodies belonging to both of the adjacent terranes; at places, mafic and ultramafic lenses are exposed

along the Indus River along this boundary of the massif. The mafic-ultramafic assemblages are possibly an extension of the Chilas stratiform complex of the Kohistan terrane probably looping around the NPHM. North of Sassi and Astak the western and eastern faults of the massif trends westward and eastward respectively. The northern extensions of the Raikot-Sassi and the Astak Faults lie beneath the Chogo Lungma glacier and it is not known yet whether the two faults join in the north to form a continuous loop around the massif or they truncate against the MKT. The anastomosing feature of the felsic dikes (aplite and pegmatite) on the island arc side of the Raikot-Sassi and Astak Faults is conspicuous.

#### BACKGROUND OF THIS STUDY

The Indus and Astore river valleys provide northeast-southwest cross-sections across the NPHM (Fig. 2). The rocks of the NPHM can be divided into psammitic gneiss, granitic gneiss, calc-silicate rock, pelitic gneiss, amphibolite, and siliceous-pegmatitic and mafic dikes. These units are interlayered with tabular bodies separated by fairly sharp contacts conformable with foliation and lithologic layering. All units, except the siliceous pegmatite dikes, have experienced kyanite/sillimanite grade metamorphism accompanied by intense deformation which has transposed original structures and modified original thicknesses. Whether the present relative position of these units or layers reflects their relative ages is not known.

The mineralogy (see below) and lithologic variation point to a sedimentary protolith for much of the gneiss in the NPHM. These sediments were formed as the continental shelf sequence at the northern margin of the Indian plate. Thick, augen-bearing, orthogneiss layers/units were probably derived from plutons that intruded the sedimentary rocks. The conform-

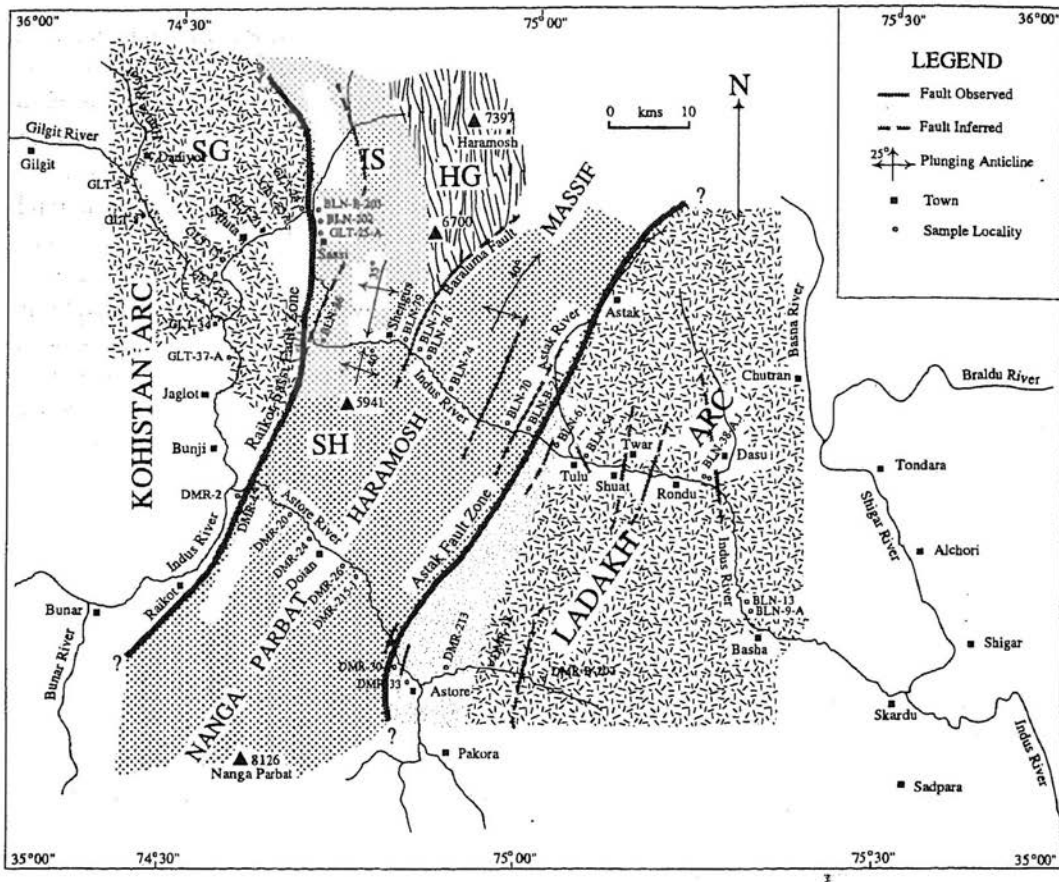


Fig. 2. Geological and sample location map of the Nanga Parbat-Haramosh Massif and the adjoining areas of the Kohistan-Ladakh arc, respectively on west and east of the massif in northern Pakistan (redrawn after Khattak & Stakes, 1993) The elevations are in meters above sea level.

able amphibolite layers probably represent basaltic material intertwined with the continental shelf sediments. Subsequently, the entire sequence was metamorphosed and deformed. The siliceous pegmatite dikes most likely represent the latest intrusive activity. The rock types included in this study are metagranite, granitic schist, amphibolite, metapelite, and tonalite (Table 1).

#### MINERAL GEOTHERMOBAROMETRY

Based on ten samples, collected from the pelitic horizons within the metasediments of the NPHM

and the adjacent portion of the Ladakh arc along the Indus and Astore rivers (Fig. 2), Khattak and Stakes (1993) and Khattak (1994), report  $\sim 725 \pm 25^\circ\text{C}$ , 8.5 kb as the peak conditions of metamorphism for the massif and the Ladakh arc. Metamorphic temperatures were determined from garnet and biotite compositions using Ferry and Spear's (1978) thermometer. Pressures were calculated using the garnet-aluminosilicate-quartz-plagioclase (GASP; Newton & Haselton, 1981) geobarometer. Pressure-temperature (P-T) histories were determined using data from studies of disequilibrium mineral textures, minerals included in garnet and zoning in the garnet. The petro-

TABLE 1. TEXTURE AND MINERALOGY OF THE REPRESENTATIVE ROCKS FROM THE NPHM AND THE KOHISTAN-LADAKH ARC TERRANES, SELECTED FOR <sup>18</sup>O ANALYSIS

Sample ID	Rock	Texture	Mineralogy (in the order of decreasing abundance)
BLN-9-A	metapelite	M,P,G	<i>qz,pg,or,bi,mus,gt,sill,opq</i>
BLN-13	metapelite	M-C,P,G	<i>qz,bi,pg,or,mus,gt,sill,opq,chl</i>
BLN-38-A	tonalite	M,G	<i>pg,qz,or,bi,sph,gt,ep,opq,ap</i>
BLN-54	amphibolite	C,E	<i>pg,hbl,bi,ep,opq,qz,ap</i>
BLN-61	tonalite	F,P,S	<i>pg,or,qz,mus,bi,gt,ap,zir,chl</i>
BLN-70	amphibolite	M,P,G	<i>pg,hbl,gt,qz,ep,bi,opq,sph,ap</i>
BLN-74	metapelite	F,P,G	<i>qz,pg,or,bi,ky,sill,mus,ep,opq,ap</i>
BLN-76	metapelite	F,P,G	<i>qz,pg,or,bi,gt,ky,mus,opq</i>
BLN-77	granitic schist	F-M,G	<i>pg,or,qz,bi,mus,spq,chl</i>
BLN-79	metapelite	F,P,G	<i>pg,qz,or,bi,mus,gt,sill,opq</i>
BLN-86	granitic schist	C	<i>pg,or,qz,bi,mus,opq</i>
BLN-202	granitic schist	F-M,P,G	<i>qz,pg,gt,bi,mus,ap,opq</i>
BLN-203	metapelite	F,P,G	<i>pg,or,qz,bi,mus,gt,ky,sill,rt,il,opq,hbl</i>
BLN-211	metapelite	F,P,G	<i>pg,or,qz,bi,gt,ky,sill,opq,ap</i>
DMR-2	amphibolite	M,S	<i>pg,bi,hbl,qz,ep,chl,opq,ap</i>
DMR-4	amphibolite	C,I,G	<i>pg,qz,chl,ep,mus,cc,sph,allan,opq</i>
DMR-20-A	granitic schist	M,S	<i>pg,qz,bi,mus,opq,ap,ep,chl,seri,zir</i>
DMR-24-B	granitic schist	M,G	<i>pg,qz,bi,mus,ap,opq,ep,sph</i>
DMR-26-A	metapelite	F,P,G/B	<i>qz,pg,or,bi,gt,mus,ky,opq,rt,ap</i>
DMR-30	granitic schist	F,P,G	<i>pg,qz,bi,gt,allan/ep,opq,sph,ap,zir,mus</i>
DMR-33-A	amphibolite	F-M,S	<i>pg,qz,hbl,bi,gt,ep,mus,opq,sph,ap</i>
DMR-38	tonalite	C	<i>pg,or,qz,mus,ep,bi,opq</i>
DMR-B-207	tonalite	C,P	<i>pg,or,qz,mus,sph,ep/allan,opq,ap</i>
DMR-213-A	amphibolite	F-M,P,G/B	<i>pg,qz,hbl,ep,bi,gt,sph,ap,chl,opq</i>
DMR-215-J	metapelite	F-M,P,G/B	<i>qz,or,pg,bi,mus,g,ky,sill,rt,il,sph,ap,opq</i>
GLT-3	metagranite	M,E	<i>pg,or,qz,mus,gt,cc,opq</i>
GLT-8	metagranite	C,I	<i>pg,or,qz,mus,bi,gt,ap</i>
GLT-13	metagranite	M,C	<i>qz,pg,or,gt,mus,bi,allan</i>
GLT-15	granitic schist	F-M,P,G	<i>qz,pg,or,bi,hbl,gt,ep,opq,ap</i>
GLT-21	metagranite	M,S	<i>pg,or,qz,bi,ep,ap,zir,rt,opq,hbl</i>
GLT-23	metagranite	C,P,G	<i>pg,or,qz,bi,mus,chl,ep,hbl,ap,zir,opq</i>
GLT-24	granitic schist	F,P,G/B	<i>qz,or,pg,hbl,bi,gt,sph,opq,cc,mus,ap,zir</i>
GLT-25-A	granitic schist	F,G	<i>pg,qz,bi,mus,ap,opq,zir,sph</i>
GLT-34	metagranite	M-C,E	<i>pg,or,qz,bi,ep,opq,allan,ap</i>
GLT-37-A	metagranite	M-C,S	<i>pg,or,qz,hbl,bi,allan,sph,ap,mus,cc</i>

Textures: B=banded; C=coarse grained; E=equigranular; F=fine grained; G=gneissose; I=inequigranular; M=medium grained; My=mylonitized; P=porphyroblastic; and S=schistose. Mineralogy: *allan*: allanite; *ap*: apatite; *bio, bi*: biotite; *cc*: calcite; *chl*: chlorite; *cor*: cordierite; *ep*: epidote; *fel*: feldspars; *gar, gt*: garnet; *hbl*: hornblende; *ky*: kyanite; *mus*: muscovite; *opq*: opaque minerals; *or*: orthoclase; *plag, pg*: plagioclase; *qtz, qz*: quartz; *rt*: rutile; *seri*: sericite; *sill*: sillimanite; *sph*: sphene; and *zir*: zircon

graphic data and the P-T estimates on core to margin garnet compositions suggest that the massif rocks followed a compressional path with increase in temperature from early to late stage of crystallization. The rocks in the Ladakh arc followed a different P-T history. The disequilibrium mineral textures and the mineral inclusions in the garnets from Ladakh and the chemical zoning in these garnets suggest that the Ladakh rocks followed a decompressional path while cooling. The P-T paths are interpreted to be the result of thrusting of the KLIA over the Indian continent along the Main Mantle Thrust (Fig. 1,2; Khattak & Stakes, 1993).

#### ANALYTICAL TECHNIQUES FOR STABLE ISOTOPE GEOCHEMISTRY

Detailed petrographic studies were conducted on 319 samples from traverses along the Indus and Astore rivers. Thirty five samples were selected for oxygen isotopic analysis of the rocks and their constituent minerals (see Fig. 2 for sample locations and Table 1 for petrographic description). A total of ninety one minerals (quartz, feldspar, garnet, biotite, muscovite and amphibole) were separated from the selected rocks and analyzed (Table 1). Standard gravimetric and magnetic techniques were used to conduct mineral separation for isotopic analysis. The rocks were crushed in a jaw-crusher to get ~0.5 cm pieces of the rock. Half of this sample was further crushed in a shatter-box for ~2-3 minutes to get a homogeneous powder for whole-rock oxygen isotope analysis. The other half was pulverized, carefully and in steps, to <700 microns (<500 microns in very fine grained rocks) size for mineral separation. This portion of the sample was sieved to get a size range of 500-700 micron grains (300-500 microns in the fine grained rocks). These mineral grains were passed through a magnetic separator for three or more times to get a workable concentrate of an individual mineral of interest.

Further mineral separation, to get a 99% or more purity level, was done by hand-picking grains under a binocular microscope. Contamination of one mineral by another was rarely found to be serious, except in the case of quartz contaminating feldspar. Consequently, only pure and well-cleaved feldspar grains were picked for analysis. Quartz samples were washed with cold, 60% hydrofluoric acid for 1-2 minutes in order to get rid of any feldspar adhering to the quartz grain.

Oxygen isotopic analyses were carried by conventional silicate extraction techniques at the University of South Carolina. An accurately weighed (10-12 mg) amount of sample was dehydrated at 55°C for 1-2 hours before loading it in high purity Ni-reaction vessel (bomb). Before adding chlorine trifluoride ( $\text{ClF}_3$ ) reagent, the sample was dehydrated at 100°C for another 1-2 hours within the bombs, constantly open to vacuum. The sample was then heated for 16-20 hours in the presence of a 10% excess amount of reagent at 600-650°C, depending on whether or not the sample was Fe-Mg-bearing (600°C in case of *Qtz*, *Fel* and *Mus*, and 625-650°C for whole rock, *Gar*, *Bio*, and *Amp*). Oxygen liberated from the silicate mineral was then allowed to react with resistance-heated graphite rod in the presence of platinum catalyst to form pure  $\text{CO}_2$  gas for mass spectrometric analysis. The mass spectrometers used are a 60° deflection instruments of the type described by Nier (1947) and McKinney *et al.* (1950). The corrections applied to the measured values are given by Craig (1957, 1961) and Garlick (1964).

Most of garnet and some quartz separates were run at the  $\text{CO}_2$ -Laser Probe Stable Isotope Laboratory at Dartmouth College in New Hampshire. The laser technique differs from a conventional one in that it uses a  $\text{CO}_2$ -Laser beam to heat the sample in the presence of an excess amount of reagent. The laser beam is manually focused and its intensity adjusted to get the

desired temperature (up to 4000°K). Bromine pentafluoride (BrF<sub>5</sub>) was used as reagent. The manifold of the line is provided with several additional cold traps to minimize fluoride and mercury contamination. The details of laser ablation used in the stable isotopic analysis are given in Sharp (1992).

The principle behind the method of oxygen isotope thermometry is the temperature dependence of the fractionation factor between two minerals. The equilibrium fractionation factor,  $\alpha_{XY}$ , between minerals X and Y is defined as  $\alpha_{XY} = (^{18}\text{O}/^{16}\text{O})_X / (^{18}\text{O}/^{16}\text{O})_Y$ , where phase X having the isotopic ratio  $(^{18}\text{O}/^{16}\text{O})_X$  is in isotopic equilibrium with phase Y with the isotopic ratio  $(^{18}\text{O}/^{16}\text{O})_Y$ , according to the reaction  $X^{16}\text{O} + Y^{18}\text{O} = X^{18}\text{O} + Y^{16}\text{O}$ , written for the exchange of only one oxygen atom. The enrichment or depletion of  $^{18}\text{O}$  in a mineral X, relative to a standard, is reported in terms of the quantity  $\delta$ , defined as:  $\delta_x = \{ [(^{18}\text{O}/^{16}\text{O})_X / (^{18}\text{O}/^{16}\text{O})_{\text{Std}}] - 1 \} * 1000$ , where  $(^{18}\text{O}/^{16}\text{O})_X$  is the 'per mil' (‰) measured ratio in mineral X. In terms of  $\delta$ -values, the fractionation factor,  $\alpha_{XY}$ , which is the ratio of  $\delta_x$  and  $\delta_y$ , becomes:

$$1000 \ln \alpha_{XY} = \frac{1 + \frac{\delta_x}{1000}}{1 + \frac{\delta_y}{1000}} - 1$$

$$= \frac{1000 + \delta_x}{1000 + \delta_y} - 1 \cong \delta_x - \delta_y = \Delta_{XY}$$

All  $\delta^{18}\text{O}$  values reported in the present research are relative to the Standard Mean Ocean Water (SMOW) redefined by IAEA in Vienna (Friedman & O'Neil, 1977). NBS-28 has a  $\delta^{18}\text{O}$  value of +9.6 on this scale. Figure 3 displays the interlab comparison of the corrected  $\delta^{18}\text{O}$  values determined for different minerals. It is clear that all the  $\delta^{18}\text{O}$  values follow the 45° line, indicating

less than 0.25 per mil interlab error, suggesting that the data are appropriate for the isotopic analysis.

## STABLE ISOTOPIC RESULTS

Table 2 lists the  $\delta^{18}\text{O}$  values of the whole rocks and the mineral separates from the study area. Among the analyzed samples, the whole rock  $\delta^{18}\text{O}_{\text{SMOW}}$  isotopic values range from 7 to 15.3‰, quartz 7.4 to 16.4‰, feldspar 7 to 16.1‰, garnet 5.3 to 13.7‰, biotite 3.9 to 12.6‰, muscovite 6.7 to 12.7‰, and hornblende amphibole from 4.4 to 7.2‰. The majority of  $\delta^{18}\text{O}$  values of minerals separated from the rocks included in this study follow the "normal" sequence. The prevalence of this sequence in many samples and the normal distribution of  $\delta^{18}\text{O}$  values among most of the constituent minerals indicates that they are in isotopic equilibrium, and are thus suitable for geothermometric analysis. The  $\delta^{18}\text{O}$  values that depart from the normal distribution (much of the feldspars, and to a lesser extent, biotite, muscovite and amphibole) are considered to represent apparent disequilibrium compositions. These isotopic modifications were probably reset by lower temperature or retrograde metamorphic equilibration or by isotopically different fluids. These values are indicated in Table 2 and Figure 4, but deleted from subsequent plots.

The whole rock and mineral  $\delta^{18}\text{O}$  values, in general, are strongly depleted along (and adjacent to) the Astak and the Raikot-Sassi Fault Zones (Fig. 2), probably indicating hydrothermal alteration by lighter waters (possibly igneous waters) in these deep (and several kilometers wide) fault zones. Another deep fault was suspected in the field at Dras and is supported by the  $\delta^{18}\text{O}$  values of sample BLN-38-A; whether or not this fault is a branch of the Astak Fault Zone is not known. Sample BLN-79 is a lower amphibolite grade metapelite and is strongly depleted. This sample occurs close to a large amphibolite band

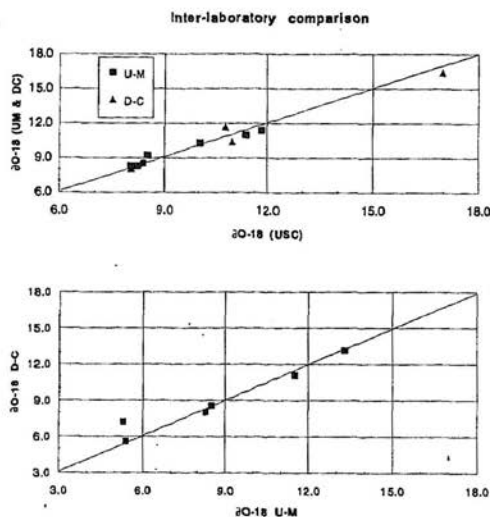
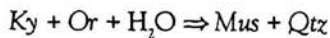


Fig. 3. Interlaboratory comparison of the corrected  $\delta^{18}\text{O}$  results of some mineral replicates and Rose Quartz standard. D-C=Dartmouth College; U-M=University of Michigan; and USC=University of South Carolina.

in the vicinity of the Baraluma Fault (Fig. 2). Away from any of the major faults, the rocks retain their high  $\delta^{18}\text{O}$  content (Fig. 5).

The majority of the samples show no petrographic evidence of re-equilibration at lower conditions other than the major upper amphibolite facies metamorphic event. Two samples, however, do show some evidence. Sample BLN-79 petrographically displays wavy grain boundaries of kyanite and back-reaction of kyanite into sericitic muscovite (Khattak, 1994), probably as:



Similarly, sample BLN-B-203 contains minor cordierite (coexisting with garnet) in its matrix assemblage which has abundant kyanite+orthoclase in it, probably indicating that the major metamorphic phase of  $\text{Ky}+\text{Or}$  was followed by much lower pressure and temperature  $\text{Cor}+\text{Gar}$  phase (Khattak, 1994; Khattak & Stakes, 1993).

The isotopic results of these samples (BLN-79 and BLN-B-203) suggest non-equilibrium values. For sample BLN-79, this disequilibrium is indicated by feldspar that is  $^{18}\text{O}$ -enriched compared to the coexisting quartz and thus not in the predicted isotopic sequence. This sample, however, is relatively  $^{18}\text{O}$ -depleted overall, and is the only metapelite to contain quartz with a  $\delta^{18}\text{O} < 8.5\text{‰}$  and garnet with a  $\delta^{18}\text{O} < 5.5\text{‰}$ . For sample BLN-B-203, the fractionation between garnet and quartz is anomalously small, suggesting an isotopic enrichment of the garnet or depletion of the quartz. Although these were the only two samples that demonstrated petrographic evidence of re-equilibration, 16 of the 35 samples had feldspar that was  $^{18}\text{O}$ -enriched compared to quartz and showed no petrographic signs of re-equilibration.

## DISCUSSION

Figure 6 is a plot showing the variation of  $\delta^{18}\text{O}$  values in  $\text{Qtz-Gar}$ ,  $\text{Qtz-Bio}$ ,  $\text{Qtz-Fel}$  and  $\text{Gar-Bio}$  pairs. Superimposed on these  $\delta$ - $\delta$  plots are lines of theoretical  $\Delta_{\text{XY}} (\cong 10^3 \ln \alpha_{\text{XY}})$  corresponding to temperatures of 500 and 700°C.  $\text{Qtz-Gar}$  pairs plot along the 700°C line, clearly indicating that this pair of minerals is contemporaneous and preserves the prograde peak temperatures of the last burial metamorphism which Khattak and Stakes (1993) have suggested to have occurred at ~8.5 kbars pressure. Since quartz and garnet are the most isotopically refractory minerals, the consistency of their  $^{18}\text{O}$  values points to metamorphic equilibration at peak temperatures. The garnets are not chloritized or amphibolitized to any degree apparent under microscope, except sample BLN-B-203, in which garnet (which has spurious  $\delta^{18}\text{O}$  value) is fractured and the fractures contain amphibole and chlorite. Trace amounts of chlorite in some samples is not associated with garnet. Quartz grains are severely strained in some of the samples

TABLE 2. WHOLE ROCK AND MINERAL  $\delta^{18}\text{O}_{\text{SMOW}}$  VALUES OF THE SELECTED SAMPLES FROM THE NPHM AND KOHISTAN-LADAKH ARC

Sample ID	W	Q	F	G	B	M	A
BLN-9-A	15.3	16.2		13.3	*12.6		
BLN-13	14.1	16.4		13.7	*11.7		
BLN-38-A	7.6	*9.8	8.4			*6.7	
BLN-54	8.3	*9.7	11.1		*5.9		
BLN-61	10.0	*10.4	9.5	7.6			
BLN-70	7.0	*9.3	8.1	5.5			*4.4
BLN-74	13.2	14.1	*13.3	11.1	*8.2		
BLN-76	10.6	11.7	9.3				
BLN-77	10.8	*12.6	*10.1				
BLN-79	9.3	*8.4	9.4	*5.3			
BLN-86	11.5	*12.0	12.7		*7.6		
BLN-202		*14.7	16.1	11.9	*7.9		
BLN-203	10.2	11.6		10.5			
BLN-211	13.3	14.7	10.4	12.0			
DMR-2	7.5	8.8	7.5				
DMR-4	8.1	*10.6	7.6				
DMR-20-A	11.1	*11.6	13.0			*9.8	
DMR-24-B	10.4	*12.0	*10.1			*9.6	
DMR-26-A	12.6		14.8	12.2			
DMR-30	9.2	10.7		7.9			
DMR-33-A	7.0	*9.2		6.3	*5.0		
DMR-38	8.8	*9.4	12.0				
DMR-B-207	8.6	*7.4	10.0				
DMR-213-A	7.5	8.3		*5.4	4.8		
DMR-215-J	11.4	*12.7	11.4	9.4	*10.1		
GLT-3	14.2	*15.3	13.5	12.3		*12.7	
GLT-8	9.5	*11.0	9.4		*6.7		
GLT-13	8.9	*9.7	7.8	*6.7	*3.9	*6.8	
GLT-15	9.9	*11.5	9.9	8.5	*7.9		
GLT-21	7.3	*8.8	7.0				
GLT-23	10.0	*10.8	12.2				
GLT-24	9.9	*11.3	13.5				*7.2
GLT-25-A	10.5	*11.6	12.9				
GLT-34	8.6	*10.3	8.6				
GLT-37-A	10.0	*11.4	9.9				*7.0

These data are plotted against northwest to southeast geographic transect of the Indus and Astore Rivers in Figure 5. W=whole rock  $\delta^{18}\text{O}_{\text{SMOW}}$  composition. All values are expressed in parts per mil (‰). The asterisked samples were run at the conventional silicate line of the University of Michigan; all garnets and the remaining quartz separates were analyzed by the Laser-ablation method at Dartmouth College; and all whole-rocks were run at the University of South Carolina. Q: quartz, F: feldspar, G: garnet, B: biotite, M: muscovite, A: Amphibole.

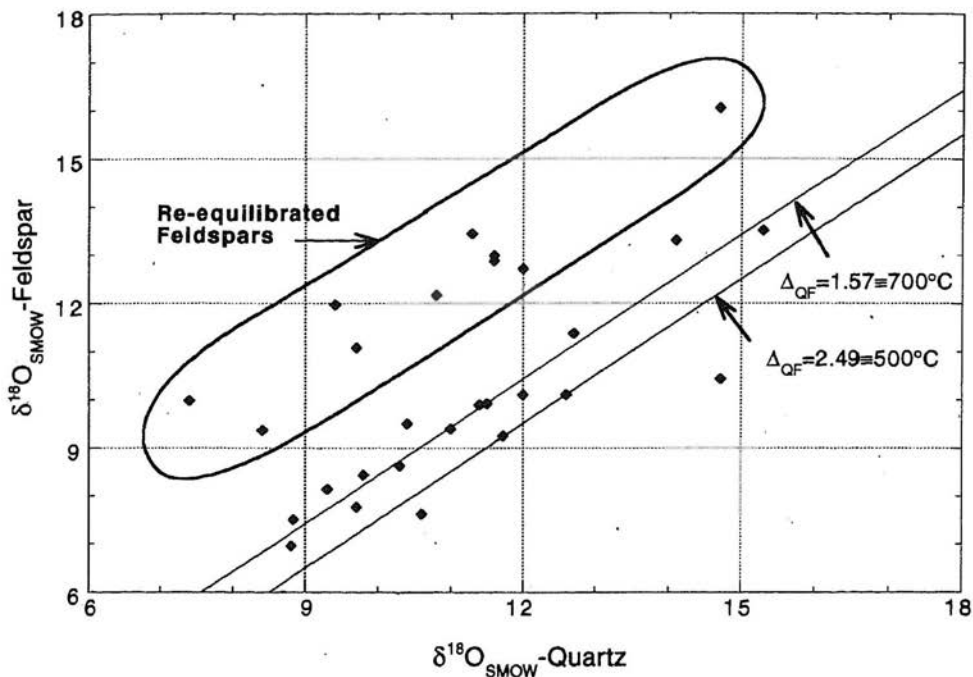


Fig. 4.  $\delta^{18}\text{O}_{\text{SMOW}}\text{-Qtz-Fel}$  plot showing reequilibrated feldspars, mostly enriched in their  $^{18}\text{O}$  composition by probably a post-metamorphic fluid activity. This fluid probably originated as formation waters resulting from the prograde metamorphic dehydration reactions occurring in sediments of the Indian plate shelf.

but none were found obviously recrystallized. The other mineral pairs are isotopically less refractory and have more variable  $\delta^{18}\text{O}$  values (Fig. 6), suggesting that some of these minerals have reset their isotopic compositions during a subsequent metamorphic event and are not useful in derivation of the peak thermal conditions of metamorphism.

Temperatures of formation are calculated using Bottinga and Javoy's (1975) calibration of

the fractionation factors and are listed in Table 3. The oxygen isotopic fractionation for fifteen of the sixteen *Qtz-Gar* pairs vary from 2.8‰ to 3.8‰ giving a range of temperatures from 764°C to 599°C respectively. The very small fractionation (1.1‰) in the remaining one pair yields a spuriously high temperature (1288°C). This sample, BLN-B-203, shows petrographic evidence of garnet recrystallization during retrograde conditions as previously discussed. The 1.0‰ variation in fractionation is greater than the expected

Fig. 5.  $\delta^{18}\text{O}_{\text{SMOW}}$ -mineral and whole rock values versus geographic cross-strike transect of the Indus and Astore rivers (NW-SE) through the NPHM in northern Pakistan. The data for this figure is tabulated in Table 3. Those values of minerals in Table 3 which did not follow the normal sequence of  $^{18}\text{O}$  enrichment were not plotted here (see text). Note strong  $^{18}\text{O}$  depletion of rocks in and around the Raikot-Sassi and the Astore Fault zones and high values in the Kohistan and Ladakh Arc rocks. The reequilibrated feldspars are deleted from this figure. Lithology of the samples is given in parentheses: 'met pel' = metapelite; 'met gra' = metagranite; 'gra sch' = granitic schist; and 'amph' = amphibolite.

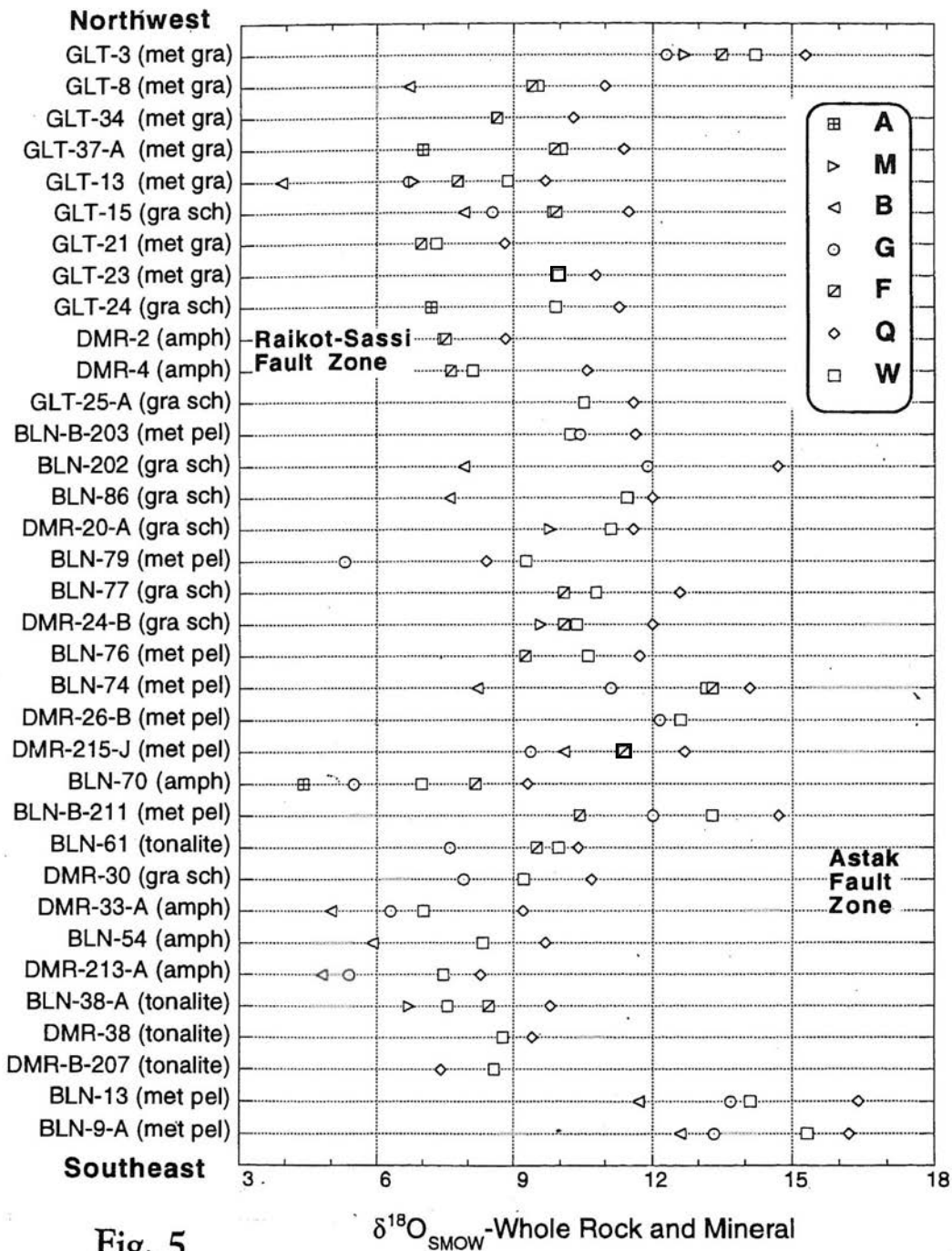


Fig. 5

error and thus indicates a real variation in the maximum temperatures. However, at temperatures of 600°C and above, the isotopic composition of a garnet is strongly dependent on its chemical composition (Valley, 1986). Microprobe analyses of these garnets show that they are almandine-rich and have essentially flat chemical zoning profiles (Khattak, 1994; Khattak & Stakes, 1993). The  $^{18}\text{O}_{\text{Qtz-Gar}}$  temperature estimates are consistent with the mineral thermometric results of Khattak and Stakes (1993). Previous workers (e.g. Chamberlain *et al.*, 1989, 1991) have suggested peak temperatures of 580°C in the massif. Our  $^{18}\text{O}$  thermometric data and Khattak and Stakes' (1993) phase equilibrium studies show that the peak temperatures must have been ~700°C.

Ten of the twelve  $\alpha_{\text{QB}}$  values range from 3.4‰ to 5.8‰ resulting in a range of temperatures from 682°C to 484°C, respectively. Two Qtz-Bio pairs have very high or very low fractionation (6.7‰ and 2.6‰) giving temperatures of 437°C and 806°C, respectively. Seven of the nine Gar-Bio pairs range in  $\alpha_{\text{GB}}$  values from 0.6‰ to 2.9‰, giving temperatures from 549°C to 208°C. One  $\alpha_{\text{GB}}$  value is very high (4‰) and one is negative (-0.7‰), both indicating disequilibrium isotopic compositions.

The massif is a complex of parallel bands and layers of different lithologies and it can be argued from the  $\delta^{18}\text{O}$  values in Figure 5 that there still exists a relationship between the chemical composition of individual band and its  $\delta^{18}\text{O}$  value. This suggests that the last metamorphism has not regionally homogenized the  $\delta^{18}\text{O}$  composition of the rocks and minerals across lithologic boundaries. Such isotopic homogenization is greatly facilitated by the availability of fluid phase present during metamorphism to cause  $^{18}\text{O}$  exchange among minerals and across lithologic barriers, especially at high temperatures. The variability

of  $^{18}\text{O}$  value of a mineral from two different lithologies within the massif refers to the fact that the studied rocks were extremely low in water content. Such an interpretation was also suggested by Khattak and Stakes (1993) based on the fact that migmatization is not common along the Indus and Astore River sections, although the temperatures and pressures (~700°C, 8.5 kbars) were high enough to melt the rocks.

A closer examination of Fig. 6 shows that the heavy as well as light Qtz-Gar pairs give a temperature estimate of 700°C. This means that the  $^{18}\text{O}$ -depletion of the lighter pairs, such as sample BLN-79, must have taken place as a pre-burial fluid activity prior to the high temperature metamorphism. This fluid caused ~3‰ depletion in the whole rock  $\delta^{18}\text{O}$  values. Such a fluid probably originated from an igneous parent. A post-burial fluid activity is evident from the heavy feldspar and the hydrous minerals (Fig. 6,7), which caused an enrichment of 3-6‰. Such a fluid probably originated from the metasediments commonly rich in  $^{18}\text{O}$  (~20‰).

Eleven of twenty-eight feldspar  $^{18}\text{O}$  values did not follow the 'normal' sequence (Hoefs, 1980) of  $^{18}\text{O}$  enrichment (Fig. 4). These feldspar values probably represent disequilibrium isotopic compositions and add a lot of scatter to the plots involving feldspar (Fig. 7, see below), consistent with previous reports suggesting that feldspar is several times more unstable of all the minerals in preserving the original isotopic abundances. Figure 7 is a plot showing the variation of  $\delta^{18}\text{O}$ -feldspar (all data) with respect to biotite, muscovite, and amphibole. This plot indicates that these minerals have apparently experienced some isotopic change after the peak of metamorphism, although there is no petrographic evidence of such a change. Most of the feldspars are optically fresh, some show bent twinning and

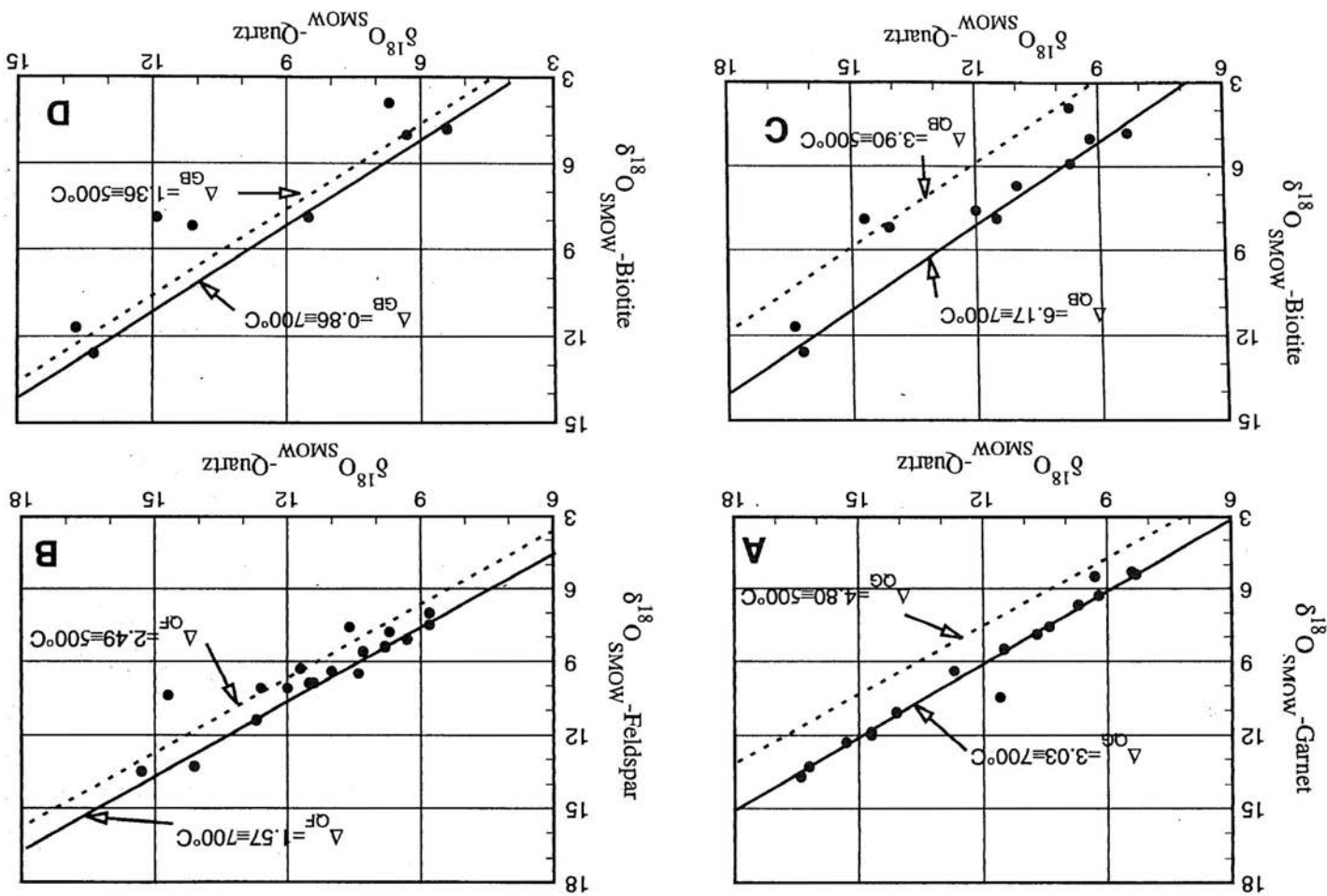


Fig. 6.  $\delta^{18}\text{O}_{\text{SMOW}}$ -mineral plots illustrating the variation of  $^{18}\text{O}$  composition and the temperatures of equilibration. A:  $\delta^{18}\text{O}_{\text{SMOW}}$ -Qtz versus  $\delta^{18}\text{O}_{\text{SMOW}}$ -Gar plot illustrating the variability of the  $\delta^{18}\text{O}$  values of the two minerals with respect to the theoretical fractionation curves for 500 and 700°C. Notice that the rocks with low  $\delta^{18}\text{O}_{\text{SMOW}}$  values still retain their  $^{18}\text{O}$  fractionation with garnet at  $\sim 700^\circ\text{C}$ , indicating that the quartz depletion took place prior to the metamorphism; B:  $\delta^{18}\text{O}_{\text{SMOW}}$ -Qtz versus  $\delta^{18}\text{O}_{\text{SMOW}}$ -Fel plot (excluding reset feldspars); C:  $\delta^{18}\text{O}_{\text{SMOW}}$ -Qtz versus  $\delta^{18}\text{O}_{\text{SMOW}}$ -Bio plot; and D:  $\delta^{18}\text{O}_{\text{SMOW}}$ -Gar versus  $\delta^{18}\text{O}_{\text{SMOW}}$ -Bio plot.

TABLE 3. TEMPERATURES (°C) OF EQUILIBRATION DERIVED FROM  $^{18}\text{O}_{\text{SMOW}}$  DATA USING BOTTINGA AND JAVOY'S (1975) FORMULATION OF MINERAL-WATER FRACTIONATIONS

Sample ID	Rock	Q-F	Q-G	Q-B	Q-M	Q-A	F-G	F-B	F-M	F-A	G-B	G-M	G-A	B-M
BLN-9-A	metapelite		736	670							507			
BLN-13	metapelite		764	567							289			
BLN-38-A	tonalite	778			501				279					
BLN-54	amphibolite	*		646				*						
BLN-61	tonalite	1018	745				588							
BLN-70	amphibolite	869	599			507	454			369			165	
BLN-74	metapelite	1079	715	484			532	315			208			
BLN-76	metapelite	506												
BLN-77	granitic schist	503												
BLN-79	metapelite	*	692				*							
BLN-86	granitic schist	*		590				*						
BLN-202	granitic schist	*	746	437			*	*			148			
BLN-B-203	metapelite		1288											
BLN-B-211	metapelite	321	764				*							
DMR-2	amphibolite	794												
DMR-4	amphibolite	438												
DMR-20-A	granitic schist	*			688				*					
DMR-24-B	granitic schist	617			587				532					

(Continued)

Sample ID	Rock	Q-F	Q-G	Q-B	Q-M	Q-A	F-G	F-B	F-M	F-A	G-B	G-M	G-A	B-M
DMR-26-B	metapolite						459							
DMR-30	granitic schist		746											
DMR-33-A	amphibolite		726	606							381			
DMR-38	tonalite	*												
DMR-B-207	tonalite	*												
DMR-213-A	amphibolite		730	682							549			
DMR-215-J	metapelite	796	660	806			562	813			*			
GLT-3	metagranite	646	714		561		811		439			1486		
GLT-8	metagranite	697		598				546						
GLT-13	metagranite	610	709	489	522		870	430	401		216	892		446
GLT-15	granitic schist	704	715	668			730	646			540			
GLT-21	metagranite	631												
GLT-23	metagranite	*												
GLT-24	granitic schist	*				576				*				
GLT-25-A	granitic schist	*												
GLT-34	metagranite	675												
GLT-37-A	metagranite	727				549				450				

The mineral-water equations were converted into mineral-mineral equations by simple mathematics. The fractionations that changed sign and the pairs that included a suspect mineral that probably had reset its  $^{18}\text{O}$  composition, represent disequilibrium and are represented by an asterisk. Q=quartz; F=feldspar; G=garnet; B=biotite; M=muscovite; and A=amphibole

contain lots of inclusions of very fine prisms of muscovite, probably indicating formation under dynamic conditions; none shows signs of recrystallization.

Two phases of equilibration are interpreted in the massif from the petrological data, a widespread upper amphibolite facies and a very local lower amphibolite facies (Khattak & Stakes, 1993). The former is evidenced by completed 'second-sillimanite' reaction; whereas the latter is inferred from the occurrence of post-kinematic muscovite, occurrence of cordierite and the absence of *Ky/Sill+Or* pair due to back reaction of this pair to *Mus+Qtz*. Both of these metamorphic events are confirmed by the stable isotopic analysis of the rocks. In addition, the  $^{18}\text{O}$  data also point to the operation of an earlier pre-burial episode of modification during which recognizable  $^{18}\text{O}$  depletion of rocks took place.

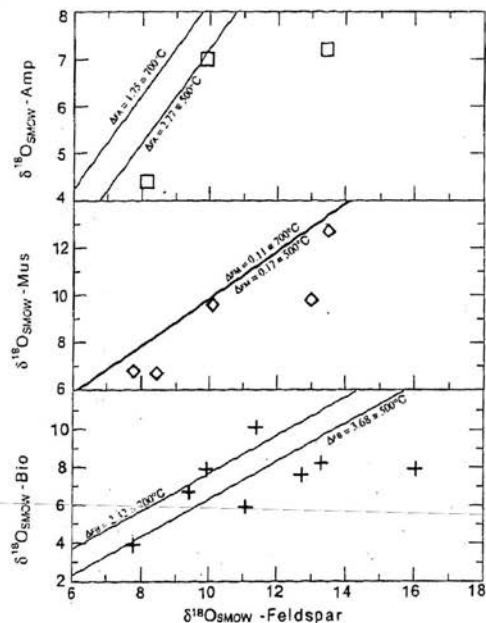


Fig. 7.  $\delta^{18}\text{O}_{\text{SMOW}} - \text{Fel}$  versus  $\delta^{18}\text{O}_{\text{SMOW}} - \text{Bio/Mus/Amp}$  plot showing heavy and light feldspar variation with the hydrous minerals.

## CONCLUSIONS

The stable isotopic results presented here provide important information on the thermal history of the Nanga Parbat-Haramosh Massif of the Pakistan Himalayas. The NPHM preserves a prograde metamorphic history which is brought about as a consequence of the collision between the Indian plate and the Kohistan-Ladakh island arc. The peak conditions of the last burial metamorphism were  $700^\circ\text{C}$ , 8.5kb, based on two independent thermometric derivations:  $^{18}\text{O}$  fractionation and Fe-Mg exchange between mineral pairs. The Fe-Mg exchange experiments are carried out at high temperatures. Due to the sluggish metamorphic reaction rates, especially involving garnet, at low temperatures, these high temperature experimental results are then extrapolated towards lower temperatures. On the other hand, the experiments involving  $^{18}\text{O}$  are done at lower temperatures, because of high fractionation at low temperature conditions, and then extrapolated to include high temperature assemblages. Identical results of temperature estimates from two totally independent methods are not coincident and represent part of the actual thermal history active during the metamorphism of the rocks.

Lack of significant migmatization along the Indus and Astore Rivers sections and total absence of granulite assemblages from the massif and the adjacent areas of Kohistan and Ladakh suggest that the temperatures were not significantly higher than  $700^\circ\text{C}$ . Low amount of water in a predominantly metasedimentary massif seems unusual, however, it is possible that much of the water from the massif rocks was squeezed out during previous metamorphic events. The absence of a petrographic evidence for such events is probably because the last upper amphibolite metamorphism obliterated all imprints of the previous episodes.

The stable isotopic geochemistry of the NPHM confirms that the quartz and garnet mineral pairs are contemporaneous and represent isotopic equilibrium. The  $^{18}\text{O}$  fractionation among quartz and garnet confirms the peak temperature of the last metamorphic episode to be  $700^\circ\text{C}$ . The *Qtz-Gar* pairs, because of their refractory physicochemical properties, best preserve the equilibration temperature of metamorphism. Some of the feldspars and OH-bearing minerals have reset their isotopic compositions after the climax of last metamorphism. The fluids prevalent subsequent to the main metamorphism probably originated from metasediments as a result of prograde metamorphic reactions. This re-equilibration probably occurred under lower amphibolite conditions ( $\sim 500^\circ\text{C}$ , 5-6 kb) supported by petrographic evidence in occasional assemblages. This interpretation indicates that these phases (i.e. feldspar, biotite, muscovite and amphibole) are mutually contemporaneous and reveal the cooling (retrograde) history of the rocks.

The stable isotopic composition of the massif and the Ladakh arc reveals important information about the amount of fluid during the last metamorphism. Isotopic exchange is supposed to be extremely vigorous at temperature of  $\sim 700^\circ\text{C}$ . The fact that the minerals and whole rocks from different lithologies within the massif and the arc retain the isotopic composition of the host rock implies that the last high grade metamorphism could not isotopically homogenize the rocks and minerals. This shows that the amount of fluid phase, necessary to cause isotopic exchange between phases, was not sufficiently available during the  $700^\circ\text{C}$  metamorphism.

#### REFERENCES

Bottinga, Y. & Javoy, M., 1975. Oxygen isotope partitioning among the minerals in igneous and meta-

morphic rocks. *Rev. Geophys. Space Phys.*, 13, 401-418.

Butler, R. W. H. & Prior, D. J., 1988. Tectonic controls on the uplift of the Nanga Parbat Massif, Pakistan, Himalayas. *Nature*, 333, 247-250.

Butler, R. W. H., Prior, D. J. & Knipe, R. J., 1989. Neotectonics of the Nanga Parbat syntaxis, Pakistan, and crustal stacking in the NW Himalayas. *Earth Planet. Sci. Letts.*, 94, 329-343.

Chamberlain, C. P., Zeitler, P., & Jan, M. Q., 1989. The dynamics of the suture between the Kohistan island arc and the Indian plate in the Himalaya of Pakistan. *J. Meta. Geology*, 7, 135-149.

Chamberlain, C. P., Zeitler, P., & Jan, M. Q., 1991. A petrologic record of the collision between the Kohistan island arc and Indian plate, northwestern Himalaya. *Geol. Soc. Am. Spec. Paper*, 232, 23-32.

Craig, H., 1957. Isotopic standards for carbon and oxygen and correction factors for mass-spectrometric analysis of  $\text{CO}_2$ . *Geochim. Cosmochim. Acta*, 12, 133-149.

Craig, H., 1961. Standards for reporting concentrations of deuterium and oxygen-18 in natural waters. *Science*, 133, 1833-.

Ferry, J. M. & Spear, F. S. 1978. Experimental calibration of the partitioning of Fe and Mg between biotite and garnet. *Contrib. Min. Pet.*, 66, 113-117.

Friedman, I. & O'Neil, J. R., 1977. *Data of Geochemistry*. Sixth Edition (M. Fleischer, ed.). USGS Prof. Paper, 440-KK.

Garlick, G. D., 1969. The stable isotopes of oxygen, in *Handbook of Geochemistry*, Vol. 2/1, p. 8/B/1-8/B/27, Springer, New York.

Hoefs, J. 1980. *Stable isotope geochemistry* (2nd ed.). Heidelberg: Springer-Verlag, 1-142.

Khattak, M. U. K., 1990. Geothermometry and Geobarometry of the Nanga Parbat-Haramosh Massif and adjoining Ladakh arc terrane, northern Pakistan. Unpubl. M.S. thesis, Univ. Washington.

Khattak, M. U. K., 1994. Petrology and stable isotope geochemistry of the Nanga Parbat-Haramosh

- Massif, northern Pakistan. Unpubl. Ph.D. Dissertation, Univ. South Carolina, U.S.A.
- Khattak, M. U. K. & Stakes, D. S. 1993. New data on the geothermobarometry of the Nanga Parbat-Haramosh Massif and adjoining Ladakh arc terrane, northern Pakistan. *Geol. Bull. Univ. Peshawar*, 26, 1-16.
- Lawrence, R. D. & Ghauri, A. A. K. 1983. Evidence of active faulting in the Chilas district, northern Pakistan. *Geol. Bull. Univ. Peshawar*, 16, 185-6.
- Madin, I., 1986. Structure and neotectonics of the northwestern part of the Nanga Parbat-Haramosh massif. Unpubl. M.S. thesis. Oregon State Univ., U.S.A.
- McKinney, C. R., McCrea, J. M., Epstein, S., Allen, H. A. and Urey, H. C., 1950. Improvements in mass spectrometers for the measurement of small differences in isotope abundance ratios. *Rev. Sci. Instrum.* 21, 724-730.
- Newton, R. C. & Hazelton, H. T., 1981. Thermodynamics of the garnet-plagioclase- $Al_2SiO_5$ -quartz geothermometer. In: *Thermodynamics of Minerals and Melts* (R. C. Newton, A. Navrotsky, & B. J. Wood, eds.). Springer-Verlag, New York, 129-145.
- Nier, A. O. C., 1947. A mass spectrometer for isotope and gas analysis. *Rev. Sci. Instrum.*, 18, 398-411.
- Peterson, M. G. & Windley, B. F., 1985. Rb/Sr dating of the Kohistan arc-batholith in the Trans-Himalaya of north Pakistan, and tectonic implications. *Earth & Planet. Sci. Lett.*, 74, 45-57.
- Powell, C. McA., 1979. A speculative tectonic history of Pakistan and surroundings: Some constraints from the Indian Ocean. In: *Geodynamics of Pakistan* (A. Farah & K. A. DeJong, eds.). Geol. Survey of Pakistan, Quetta, 5-24.
- Sharp, Z. D., 1992. In situ laser microprobe technique for stable isotope analysis. *Chemical Geology (Isotope Geoscience)* 101, 3-19.
- Valley, J. W., 1986. Stable isotope geochemistry of metamorphic rocks. In: *MSA Reviews in Mineralogy* (J. W. Valley, H. P. Taylor, Jr., J. R. O'Neil, eds.). 16, 445-489.
- Verplanck, P. L., 1986. A field and geochemical study of the boundary between the Nanga Parbat Haramosh massif and the Ladakh arc terrane, northern Pakistan. Unpubl. M.S. thesis, Oregon State University, U.S.A.
- Zeitler, P. K., Sutter, J. F., Williams, I. S., Zartman, R., & Tahirkheli, R. A. K., 1991. Geochronology and temperature history of the Nanga Parbat-Haramosh massif, Pakistan. *Geol. Soc. Am. Spec. Pap.*, 232, 1-22.
- Zeitler, P. K., Tahirkheli, R. A. K., Naeser, C. W., & Johnson, N. M., 1982b. Unroofing history of a suture zone in the Himalayas of Pakistan by means of fission track annealing ages. *Earth Planet. Sci. Lett.* 57, 227-240.